Available online at www.sciencedirect.com
ScienceDirect
Nuclear Instruments and Methods in Physics Research A 569 (2006) 488–491
NUCLEAR INSTRUMENTS & METHODS IN PHYSICS RESEARCH Section A
www.elsevier.com/locate/nima

Preliminary assessment of the imaging capability of the YAP–(S)PET small animal scanner in neuroscience

Antonietta Bartoli[a,*], Nicola Belcari[a], Daniela Stark[b], Sabine Höhnemann[b], Markus Piel[b], Marc Jennewein[b], Ulrich Schmitt[c], Julia Tillmanns[d], Oliver Thews[d], Christoph Hiemke[c], Frank Roesch[b], Alberto Del Guerra[a]

[a]*Department of Physics "E. Fermi" and Center of Excellence "AmbiSEN", University of Pisa, and INFN, Sezione di Pisa, Pisa I- 56127, Italy*
[b]*Institute of Nuclear Chemistry, University of Mainz, Mainz D-55099, Germany*
[c]*Department of Psychiatry, University of Mainz, Mainz D-55099, Germany*
[d]*Institute of Physiology and Pathophysiology, University of Mainz, Mainz D-55099, Germany*

Available online 6 October 2006

Abstract

The new and fully engineered version of the YAP–(S)PET small animal scanner has been tested at the University of Mainz for preliminary assessment of its imaging capability for studies related to neuropharmacology and psychiatry. The main feature of the scanner is the capability to combine PET and SPECT techniques. It allows the development of new and interesting protocols for the investigation of many biological phenomena, more effectively than with PET or SPECT modalities alone. The scanner is made up of four detector heads, each one composed of a $4 \times 4\,cm^2$ of $YAlO_3$:Ce (or YAP:Ce) matrix, and has a field of view (FOV) of 4 cm axially $\times$ 4 cm $\varnothing$ transaxially. In PET mode, the volume resolution is less than $8\,mm^3$ and is nearly constant over the whole FOV, while the sensitivity is about 2%. The SPECT performance is not so good, due to the presence of the multi-hole lead collimator in front of each head. Nevertheless, the YAP–PET scanner offers excellent resolution and sensitivity for performing on the availability of D2-like dopamine receptors on mice and rats in both PET and SPECT modalities.
© 2006 Elsevier B.V. All rights reserved.

PACS: 87.58.Fg; 87.58.Ce; 87.57.Ce; 87.58.Ji

Keywords: Small animal scanner; YAP–(S)PET spatial resolution; Sensitivity; Brain imaging; Dopaminergic receptor availability

1. Introduction

The use of nuclear medicine techniques (as PET and SPECT) in small animal studies has undergone a significant increase in recent years due to the development of dedicated scanners [1,2]. Clinical scanners do not provide adequate resolution and sensitivity for small animal investigations [3]. One of the latest achievements in this area is the YAP–(S)PET scanner. It was originally developed [4,5] at the Department of Physics of the Universities of Ferrara and Pisa, and is now commercially available [6]. The YAP–(S)PET is the only scanner that combines the PET and SPECT techniques and offers the unique possibility of developing new protocols for the investigation of many biological phenomena more effectively than with PET or SPECT modalities alone [7,8]. Here, we present an example of the main performance of the fully engineered version of the YAP–(S)PET.

The scanner was tested at the University of Mainz for preliminary assessment of its imaging capability for studies related to dopamine D2/D3 receptors. Initial results obtained with ^{18}F–Fallypride (^{18}F–FP) and ^{123}I-N-allyl-epidepride (^{123}I–NAE) performed both in PET and SPECT using rats and mice are presented.

2. The YAP–(S)PET scanner architecture

The scanner is made up of four detector heads, each one composed of a $4 \times 4\,cm^2$ $YAlO_3$:Ce (or YAP:Ce) matrix of

*Corresponding author. Tel.: +39 050 2214940; fax: +39 050 2214333.
E-mail address: bartoli@df.unipi.it (A. Bartoli).

0168-9002/$ - see front matter © 2006 Elsevier B.V. All rights reserved.
doi:10.1016/j.nima.2006.08.146

20×20 crystals. Each crystal is $2 \times 2 \times 25\,mm^3$ and is optically insulated by a 5 μm reflecting layer. The matrix is directly coupled to a position sensitive photomultiplier (PS–PMT, Hamamatsu R2486) with 3 in ∅ and 0.5 mm of intrinsic spatial resolution. The four modules are positioned on a rotating gantry (see Fig. 1) and opposing detectors are in time coincidence when used in PET mode. The switch to SPECT modality can be made by replacing the tungsten septum (used in PET for shielding the detector from the background outside the FOV) with a high-resolution parallel-hole lead collimator (0.6 mm ∅, 0.15 mm septum, 2 cm thick). For both modalities, the scanner has an axial and transaxial field of view (FOV) of 4 cm. The system can operate in 2D (PET and SPECT) and 3D data acquisition mode (only PET mode). Both FBP (Filtered Back Projection) and EM (Expectation Maximization) algorithms [9] can be used for image reconstruction.

3. Performance evaluation

This paper presents just the YAP–(S)PET spatial resolution and sensitivity for both PET and SPECT modalities; other performance can be found in [10].

3.1. Spatial resolution

In PET mode, a 370 kBq ^{22}Na point-like source, embedded in a plastic disk and with 1 mm nominal size diameter was used to measure axial (A), radial (R) and tangential (T) (FWHM of the image peak) resolution of the scanner. The point source was positioned at different radial distances from the scanner axis with a 5 mm step size. In SPECT mode, a ^{99m}Tc source positioned parallel to the FOV axis with 1 cm radial offset was used. The inner tube diameter was 0.8 mm, the outer one was 1.2 mm. The radial and tangential FWHM have been measured using an energy window of 140–250 keV.

The spatial resolution was evaluated using both EM and FBP (ramp filter) algorithms. In PET mode, the 3D sinograms were reduced to 2D via multi-slice rebinning (3D-MS), while in SPECT mode the sinograms are intrinsically 2D. For EM algorithm the number of iterations was determined by an empirical parameter [9]. The image matrix voxel size was $0.5 \times 0.5 \times 2\,mm^3$ in both modalities.

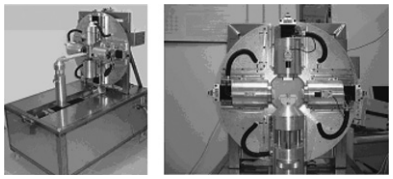

Fig. 1. Photograph of the YAP–(S)PET scanner (left) and zoom of the four rotating heads (right).

3.2. Sensitivity

In PET mode, absolute sensitivity measurements were performed with a 200 kBq ^{22}Na point-like source. The point source was placed in the center of the FOV and moved along the axis. An energy window of 50–850 keV was used. The β^+ decay branching ratio of ^{22}Na (0.9055), and the system dead time were accounted for. SPECT sensitivity measurements were performed with a syringe filled with a calibrated activity of ^{99m}Tc. An energy window of 140–250 keV was used.

3.3. Derenzo phantom studies

The sizes of the Derenzo rods were 3.0, 2.5, 2.0, and 1.5 mm ∅. The center-to-center distance between adjacent rods was twice the rod diameter. In PET mode, the phantom was filled with 11 MBq of a ^{18}F–FDG solution, and scanned for 75 min. A wide-open energy window (50–850 keV) and both EM and FBP (ramp filter) algorithms were used. In SPECT mode, the same Derenzo phantom was filled with 110 MBq of ^{99m}Tc and scanned for 5 h. The energy window of 140–250 keV and both algorithms were used.

4. Results

4.1. Spatial resolution

In PET mode, the highest volume resolution is measured at the center of the FOV (CFOV) using EM reconstruction. The FWHM is $1.52 \times 1.62 \times 2.10$ mm (R × T × A): volume resolution $5.2\,mm^3$. No source dimension subtraction was made. With FBP the measured resolution at CFOV is $1.97 \times 2.21 \times 2.18$ mm (R × T × A) ($9.5\,mm^3$). In SPECT mode, the spatial resolution is constant over the whole FOV, and the FWHM image profile in the transaxial plane is 3.1×2.9 mm (R × T) using EM algorithm and 3.9×4.1 mm using FBP algorithm. Detailed spatial resolution graphs are reported in [10,11].

4.2. Sensitivity

In PET mode, the maximum absolute sensitivity, measured at CFOV, was 1.87% (18.7 cps/kBq) for an energy window of 50–850 keV. In SPECT mode, the sensitivity in the 140–250 keV energy window is constant over the whole FOV and is 30 cps/MBq.

4.3. Derenzo phantom studies

Fig. 2 shows the comparison between PET and SPECT Derenzo phantom image reconstruction using EM algorithm. Fig. 2(a) is obtained in PET mode and emphasizes the scanner capability to clearly resolve all Derenzo hot spots, including the 1.5 mm diameter rods.

Fig. 2. From the right moving anti-clock wise we have 3.0, 2.5, 2.0 and 1 mm diameter holes. (a) PET image obtained with EM algorithm (50–850 keV). (b) Photograph of the Derenzo phantom. (c) Reconstructed image in SPECT: EM algorithm (140–250 keV).

5. Animal studies

In order to evaluate the YAP–(S)PET imaging capabilities for studies related to dopamine D2/D3 receptor, a series of experiments were carried out at the University of Mainz, Nuclear Chemistry Institute.

The ^{18}F–FP, was used in PET mode on normal rats; the ^{123}I–NAE in SPECT modality, was evaluated on mice.

5.1. Materials and methods

5.1.1. Synthesis

^{18}F–FP. The tosylated precursor (5 mg, 10 μmol) was dissolved in 1 ml acetonitrile, treated for 5 min at 65 °C with potassium carbonate (5 mg, 36 μmol) and transferred into a 5 ml vial containing ^{18}F-Fluoride. The reaction mixture was heated for 20 min at 85 °C, diluted with 1 ml phosphoric acid (10%) and separated using HPLC 250(10, RP8, CH3CN: 0.25 M ammonium acetate buffer + 5 ml acetic acid/l 30:70, 5 ml/min). The fraction containing ^{18}F–FP was isolated, diluted with 0,15 M disodium hydrogen phosphate buffer and adsorbed on a ^{18}C cartridge in order to remove the HPLC solvent. The column was washed with 2 ml water and eluted with 1 ml ethanol. The solvent was removed in vacuo, and the ^{18}F–FP resolubilized with 2 ml of an isotonic sodium chloride solution, containing 1% sterilely filtrated DMSO. Before injection, quality control was performed including chemical and radiochemical purity, specific activity, pH and absence of pyrogens.

^{123}I–NAE. The iodinated analog of ^{18}F–FP, N-allyl-epidepride (^{123}I–NAE) was prepared from its stannous precursor in an eppendorf vial, using acidic conditions for its radioiodination. The precursor (50 μg/25 μl ethanol), 20 μl of ^{123}I–NaI (3.4 GBq/210 μl) in NaOH (pH 12–13), ZAG Karlsruhe, 3 μl 2 N HCl and 10 μl CAT (1.5 mg/ml) in water, were reacted for 10 min. The reaction mixture was injected into the HPLC system (described below). The activity peak corresponding to the product was collected, diluted with acetonitrile/water, fixated on a ^{18}C cartridge and eluted with ethanol. The ethanol was removed in vacuo and the residue taken up in isotonic saline solution containing 1% DMSO. 300 μl were injected into the mouse containing 28 MBq ^{123}I–NAE. ^{123}I–NAE was purified using HPLC with acetonitrile/ammonium acetate buffer (0.25 M) acidic acid added to pH 4.5 as eluent (gradient: 70/30 buffer/MeCN to 90/10 over 20 min after ten minutes of isocratic flow at 70/30; HPLC column: SDV 10000 10 μ/125 × 4 mm) Polymer Standards Service GmbH, flow rate 0.5 ml/min.

5.1.2. PET and SPECT scanning

The PET studies were applied to two groups of healthy male rats (CD, 300 g). One group was treated with an intraperitoneal injection of 50 mg/kg (body weight) amisulpride in order to block the binding of the ^{18}F–FP; the other one was not treated. All the animals were anesthetized with chloralhydrate 7%, injected via a lateral tail-vein with 37 MBq of ^{18}F–FP and immediately scanned with a dynamic protocol: 5 × 1.5 min, 5 × 2.5 min and 10 × 7 min acquisitions. The images were reconstructed using EM algorithm with 40 iterations: voxel size of 0.5 × 0.5 × 2 mm (R × T × A). Reconstruction does not include scatter and attenuation corrections.

In SPECT mode, the mice were intravenously injected with 28 MBq of ^{123}I–NAE and scanned for a few hours.

5.2. Results

The upper part of Fig. 3 shows a transaxial (left) and a coronal (right) slice of a normal rat, injected with 37 MBq of ^{18}F–FP. The lower part shows a transaxial (left) and a coronal (right) slice of a rat, treated with dopamine receptor antagonist. The scanner resolution in PET mode allows to clearly distinguish between the right and left striatum. Images obtained with receptor blocking clearly indicate the specific binding of ^{18}F–FP to D2-like receptors in the rat brain. The sensitivity of the scanner permitted the generation of a rough time-activity curve (Fig. 4). Quantitative data analysis is still under development, so the *y*-axis reports activity in arbitrary units. The graph was obtained by evaluating the number of counts in the selected region-of-interest (ROI): left and right striatum, cerebellum and skull. ROIs were drawn on summed slices (2–3 slices,

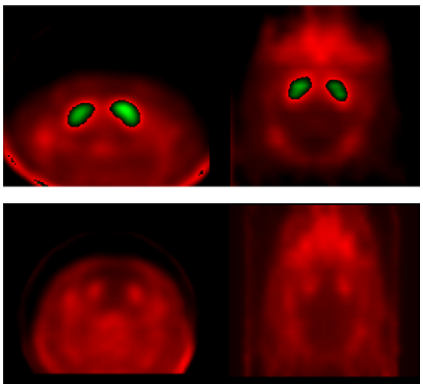

Fig. 3. Transaxial (left) and coronal (right) slices of a healthy male rat (upper figure) and of a male rat treated with amisulpride (lower figure). Voxel size: 0.5 mm × 0.5 mm × 2 mm (R × T × A). EM algorithm with 40 iterations was used.

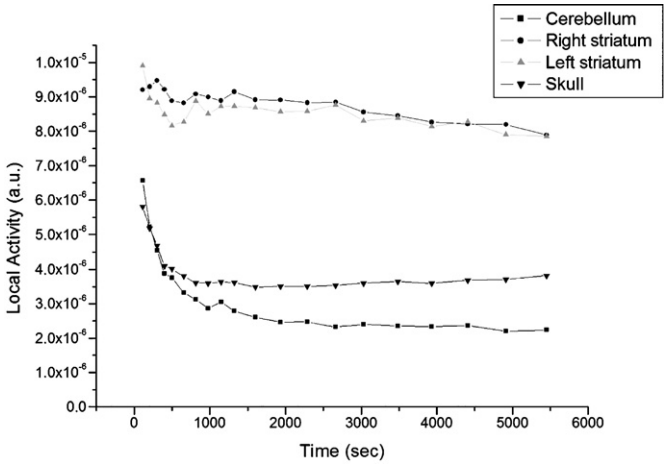

Fig. 4. Rough quantitative time activity curves (the activity on y-axis is in arbitrary units) of the dynamic study of a healthy male rat. Right and left striatum, cerebellum and skull were evaluated.

Fig. 5. Transaxial slice (0.5 mm × 0.5 mm pixel dimensions, 2 mm thick) of a normal mouse. EM algorithm with 20 iterations was used. The right and left striatum can be clearly discriminated.

2 mm each) to improve the signal to noise ratio and to reduce the partial volume. Fig. 4 highlights the difference between the strong ^{18}F–FP binding in the rat striata and the fast wash-out in the cerebellum, which is considered as a non specific binding. In Fig. 5 a transaxial section of a SPECT acquisition on a mouse with ^{123}I–NAE is shown. The image is not very clear, due to two main aspects: the thickness of YAP–(S)PET scanner collimators and the reduced dimension of the mouse striatum. In contrast to ^{99m}Tc imaging, the thickness of the collimators is not enough to stop the small percent (1–2%) of high energy radiation (around 520 keV) emitted by ^{123}I, whose Compton interaction in the crystals produces a nearly uniform background below the 159 keV photopeak. It was therefore necessary to elaborate a subtraction procedure. As a first approximation we considered the background underneath the peak (135–230 keV energy window), B_{SA}, as a fixed fraction (f) of the counts measured in an energy window (230–370 keV), SB, close to the photopeak but containing only Compton events. In order to estimate this fraction, we performed an acquisition with a collimator replaced by a "no-hole collimator" (a lead block) and calculated the ratio f between the sinogram contents in the two energy windows. For a more accurate evaluation, the ratio was obtained by dividing pixel by pixel, the two sinograms and averaging the result over the angle coordinates. Thus f becomes a matrix. The "corrected" sinogram used for image reconstruction was obtained by subtracting $B_{SA}(= f*SB)$ from the image sinogram, evaluated in the energy window 135–230 keV.

The mouse striatum dimension is at the limit of the SPECT scanner spatial resolution.

6. Conclusion

Preliminary assessment of imaging capability for studies related to dopamine D2/D3 receptor were performed at the University of Mainz with the fully-engineered version of the YAP–(S)PET scanner.

The PET studies, realized by injecting rats with ^{18}F–FP and monitoring both the striatum and cerebellum activity distributions with dynamic acquisitions, showed an excellent scanner resolution and sensitivity. The SPECT studies performed on mice with ^{123}I–NAE exposed some more difficulties due to the thickness of the scanner collimators and the reduced dimension of the mouse striatum. Nevertheless the obtained images emphasized the YAP–(S)PET capability in performing good quality PET and SPECT dopamine receptor studies.

Acknowledgments

This work was supported in part by European Molecular Imaging Laboratories (EMIL) grant LSHC-CT-2004-503569. The authors would like to thank Dr. D.J. Herbert and Dr. F. Landini for their assistance in preparing the manuscript.

References

[1] A. Chatziioannou, Eur. J. Nucl. Med. 29 (2002) 98.
[2] A. Del Guerra, et al., Q. J. Nucl. Med. 46 (1) (2002) 35.
[3] A. Del Guerra, et al., Nucl. Instr. and Meth. A 513 (2003) 13.
[4] A. Del Guerra, et al., Nucl. Instr. and Meth. A 409 (1998) 537.
[5] A. Del Guerra, et al., IEEE Trans Nucl Sci 47 (2000) 1537.
[6] http://www.ise-srl.com/YAPPET/YAP-PET.htm.
[7] A. Bauman, et al., "First evaluation of uptake kinetics of the 18F-labelled dopamine neurotransmitter analogue 18F-Fallypride using the YAP–(S)PECT small animal imager", 2005 internal report, unpublished.
[8] A. Del Guerra, et al., "Simultaneous PET/SPECT imaging with the small animal YAP–(S)PET scanner", presented at the 2002 annual conference of the Academy of Molecular Imaging, October 23–27, 2002, San Diego, CA, (USA) (abstract).
[9] A. Motta, et al., Comp. Med. Im. Graph 26 (2002) 293.
[10] A. Del Guerra, et al., IEEE Trans. Nucl. Sci. 53 (2006) 1078.
[11] A. Vaiano, Calibration an performance of the small animal PET/SPECT scanner YAP–(S)PET, Speciality school of Medical Physics Thesis, University of Pisa, 2004, unpublished.